

We are IntechOpen, the world's leading publisher of Open Access books Built by scientists, for scientists

6,900

Open access books available

186,000

International authors and editors

200M

Downloads

Our authors are among the

154

Countries delivered to

TOP 1%

most cited scientists

12.2%

Contributors from top 500 universities



WEB OF SCIENCE™

Selection of our books indexed in the Book Citation Index
in Web of Science™ Core Collection (BKCI)

Interested in publishing with us?
Contact book.department@intechopen.com

Numbers displayed above are based on latest data collected.
For more information visit www.intechopen.com



Life Time Analysis of MCrAlY Coatings for Industrial Gas Turbine Blades (calculational and experimental approach)

Pavel Krukovsky¹, Konstantin Tadlya¹, Alexander Rybnikov²,
Natalya Mozhajsckaya², Iosif Krukov² and Vladislav Kolarik³

¹*Institute of Engineering Thermophysics, 2a, Zhelyabov Str., 03057 Kiev*

²*Polzunov Central Boiler and Turbine Institute, 24, Politechnicheskaya Str.
194021 St. Petersburg*

³*Fraunhofer-Institut für Chemische Technologie, 7, Joseph-von-Fraunhofer Str.,
76327 Pfinztal*

¹*Ukraine*

²*Russia*

³*Germany*

1. Introduction

Modern power gas turbine blades are subject to high-temperature oxidation and are protected by metal coatings of MCrAlY type. The major element retarding oxidation of a coating is aluminium (Al) whose percentage in a coating amounts to 6-12%.

A blade coatings lifetime of 25000 h is required in stationary gas turbines at operating temperatures from 900 to 1000 °C making experimental lifetime assessment a very expensive and often a not practicable procedure. A feasible and low-cost method of coating lifetime assessment is the calculation analysis (modeling) of mass transfer processes of basic oxide-forming elements (in our case Al) over a long period of time. Oxidation (Al_2O_3 oxide film forming on the external coating surface) and Al diffusion both towards the oxide film border and into the basic alloy of a blade are the mass transfer processes which determine coating lifetime at the usual operating temperatures.

The existing models describing high-temperature oxidation and diffusion processes in MCrAlY coatings use simple approximated empirical dependences (of power-or other type) [1-4] for oxide film mass or thickness variation with time, and differential equations describing the oxide-forming element diffusion in the «oxide-coating-basic alloy» system [5, 6].

However the practical application of these models for long-time prediction is often difficult or impossible because of the lack of reliable model input parameter values, such as diffusion factors of an oxide-forming element. Some data on element diffusion factors can be found in literature only for simple alloy compositions (two- or three-component alloys), while the alloys used in practice are more complex. In the present case a coating alloy containing 5 elements-nickel, cobalt, chromium, aluminium, yttrium – is to be investigated. Data on Al diffusion factor can be found in literature studying similar element composition, but only for three-component NiCrAl alloy [7].

It should be noted that the models, which have been described in [5, 6] disregard the importance of a number of alloys peculiarities of Al transport from the coating to the base alloy, which is, the formation of a so-called interdiffusion zone between the coating and the base alloy. In that case mass transfer from the coating to the base alloy occurs through the interdiffusion zone and the Al accumulation here begins to play an important role. The factors of its mathematical description become all the more uncertain.

This work offers to define model factors (effective Al diffusion factor, the intensity factor of aluminum segregation in the interdiffusion and other zones) using the solution of inverse problems of diffusion based on the experimental data on Al concentration distributions at different coated sample exposure times and temperatures in furnaces. The approach based on the use of short-term experimental data for model factor determination followed by the application of this model for long-term predictive calculations is called here as a calculation-experimental approach.

This approach was used for the analysis of chromium mass transfer in a coating with the formation of chromium oxide and chromium diffusion into a basic alloy [8] except for the coating life analysis.

The purpose of this work is to improve the existing model of mass transfer processes in MCrAlY-type metal coatings as well as the development and application of the calculation-experimental approach to coating life assessment based on the proposed models and the solution of inverse problems of diffusion.

2. Calculational and experimental approach

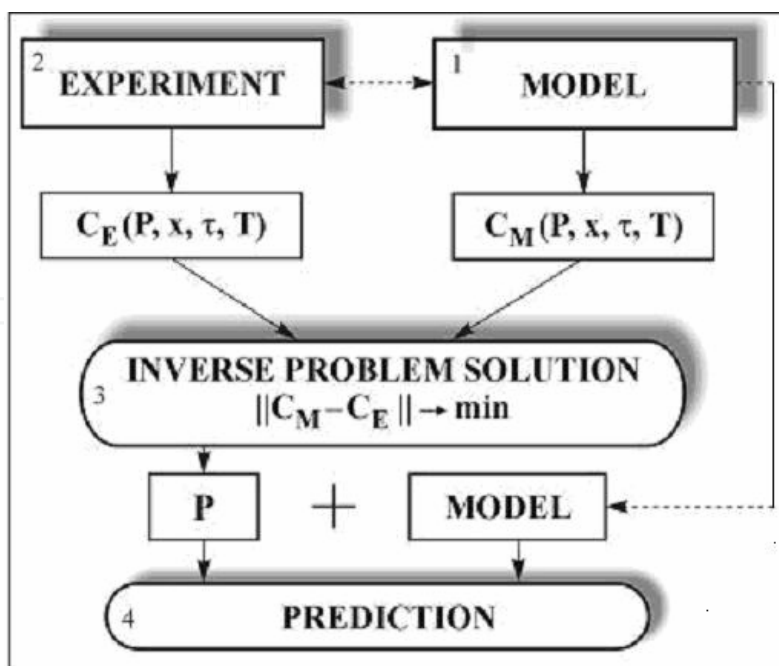
The essence of the present approach is the choice of such a mass transfer model and a set of data which, when combined, enable one to obtain a more equivalent model based on the solution of inverse problems of diffusion (IPD). The use of the model will allow for a more accurate long-term prediction of mass transfer processes and metal coating life at given lifetime criterion.

The diagram of the approach (Fig.1) to mass transfer prediction is as follows:

1. The construction (selection) of a mathematical model which gives the adequate description of major physical processes occurring in the system under consideration and determining coating life. This model makes it possible to find the calculated C_m concentration (profiles) for Al in the coating-basic alloy system.
2. The performance of short-term experimental studies in order to find regular trends of the oxide film and interdiffusion zone formation and determine Al concentration distributions in a coating and a basic metal (C_E) at different times and temperatures (coated sample exposures in furnaces).
3. The identification of the unknown $P_n(T)$ model parameters from experiments based on the IPD solution, which gives the proximity of C_M and C_E profiles by minimizing the F value.
4. Long-term prediction of mass transfer processes and coating life with the use of the proposed model in p.1 together with the unknown model parameters determined in p.3.

A simpler diagram of prediction is usually used (Fig.1): model + literature $P_0(T)$ model parameters = prediction.

Generally the diagram can be applied for simple alloy compositions, for instance, for a three-component alloy [5, 6]. As for more complex compositions, it may lead to insufficiently accurate predictions due to the uncertain $P_0(T)$ model parameters. So the use of a full calculation-experimental approach diagram based on the identified $P_n(T)$ model parameters provides more accurate predictions.



1 Experiment, 2 Model, 3 Inverse Problem Solution, 4 Prediction

Fig. 1. Diagram of the calculation and experimental approach to mass transfer and life predictive of gas turbine blade coatings.

The calculation-experimental approach under consideration suggests a search (identification) for model parameters (p.3) by means of IPD solution based on the available short-term experimental data. The IPD solution amounts to searching for such $P_u(T)$ parameter values for which the quantity

$$F = \left\{ \sum_{j=1}^m [C_{j,M}(P(T)) - C_{j,E}]^2 / m \right\}^{0.5} \rightarrow \min \quad (1)$$

This method of IPD solution is given in more detail in [8, 9]. Thus the calculation-experimental approach manifests itself as a way of improving the accuracy of the results of calculations and prediction of the processes at hand by identifying the mathematical model parameters based on the experimental data on the process being studied. The construction of the mathematical model required the performance of special works concerned with the study of the regularities of high-temperature material and coating behaviour during long-term exposures at high temperatures and the development of a physically valid model for coating life prediction.

3. Experiment

In this connection the purpose of short-term researches was a study of kinetics of the oxide film formation on a coating surface, structural changes in surfaces layers of coated heat-resistant alloys, and the modeling of structural-phase changes in coatings and at isothermal ageing the duration of which was sufficient for model parameter identification. Then the experiment was continued till coating life expiration in order to confirm the validity of the proposed method.

The work investigated the degradation of two coatings with different aluminum content. The coatings were applied on IN 738LC alloy samples by LPPS (Low Pressure Plasma Spray) method. The isothermal exposure times and temperatures are given in Table 1.

| Coating | Coating thickness, μm | Base material | Exposure temperature, $^{\circ}\text{C}$ | Exposure time, hr |
|-----------------|----------------------------------|---------------|--|--|
| Ni30Co28Cr8AlY | 100 | IN 738 LC | 900, 950, 1000 | 100, 300, 700, 1000, 5000, 10000, 15000, 20000 |
| | 200 | | | |
| Ni30Co28Cr10AlY | 100 | IN 738 LC | 900, 950, 1000 | 100, 300, 700, 1000, 5000, 10000, 15000, 20000 |
| | 200 | | | |

Table 1. The program of coated sample tests.

The samples of the same thickness and composition were obtained by cutting cylindrical bar (10 mm in diameter and 100 mm long) into pieces. The isothermal oxidation in air was carried out in laboratory muffle furnaces (LINN HIGH TERM LK 312-type) equipped with parameter control system (PID-controls) allowing to put the furnace into a specified mode and maintain the required temperature. Initial samples and those after isothermal exposure were subjected to metallographic examination by optical microscopy, X-ray spectrum microanalysis and X-ray diffraction analysis for studying the changes which had occurred in coatings. The samples were electropolated with Cu before preparation (cutting, mechanical grinding and polishing) in order to preserve the oxide film which had formed on a coating surface after exposure in the furnace.

3.1 Metallographic examination

The inverted microscope «Neophot 32» (Karl Zeiss Jena) with the «Baumer Coptronic» video camera was used for the micrographic examination. The obtained images were processed by means of «VideoTest Structure» software («Video Test», St. Petersburg, Russia). The following parameters were measured on each sample with the use of digital metallography:

- thickness of an oxide film and all layers formed in a coating and adjacent basic metal layer as a result of isothermal exposure in air;
- the volume fraction of phases existing in an initial coating and formed during isothermal exposure.

3.2 X-ray spectrum microanalysis

The X-ray spectrum microanalysis was carried out using MS46 «Camera» X-ray spectroscope analyzer. Samples before etching and poorly etched were used for study. The standards of both pure metals and compounds and known-composition alloys have been used for quantitative concentration evaluations of elements under consideration. The corrections for absorption, atomic number and characteristic radiant fluorescence effects were introduced by using special computer program. The curve for aluminium concentration variation across the depth of a coating and basic metal layer was built after each exposure. To this end, the X-ray spectrum microanalysis of coating and basic metal layers was carried out every 2 to 10 μm and up to 250 μm deep. The window size for the element analysis was 100 μm parallel and 3 μm perpendicular to the coating surface (100 \times 3 μm).

3.3 X-ray diffraction analysis

The oxide film formation in the first 100 hours was studied in situ by high-temperature X-ray diffraction by Fraunhofer Institute for Chemical Technology, Germany.

The experimental set-up consists of an X-ray diffractometer and a high-temperature device with a programmable thermal controller. A set of X-ray diffraction patterns with a defined time interval or temperature step was recorded in situ allowing for the identification of structural changes in the sample as a function of time or temperature. This method makes it possible

- to identify in-situ the following oxide phases,
- To follow the formation of each phase in time or as a function of temperature;
- To evaluate kinetic data on each of the reactions involved;
- To detect the thermal expansion of all phases simultaneously;
- To determine residual stresses in the oxide film or basic metal.

In order to identify the oxide phase structures ex situ after long term exposures, the X-ray diffraction analysis was performed using a DRON-3M diffract meter in Cu K α radiation with corresponding filters. Methods of polycrystalline sample structure examination were standard.

3.4 Experimental results

3.4.1 Protective oxide film formation mechanism

The mechanism of oxide film formation and growth on coating surfaces after long exposures at high temperatures in air or pure fuel combustion products was studied (Fig.2).

Oxidation measurements were carried out on coating under isothermal conditions (900°C, 950°C and 1000°C) up to 20000 hours.

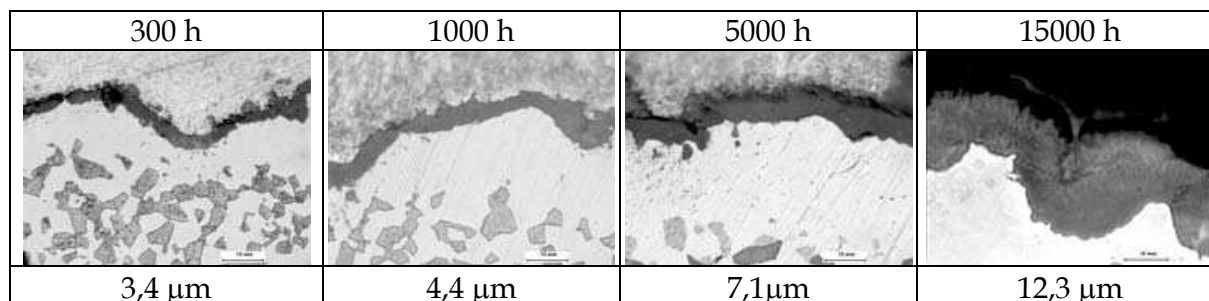


Fig. 2. Oxide film thickness on a coating surface depending on time of isothermal oxidation

The measurement of oxide film thickness after different exposure times show that the change in oxide film thickness at the initial stage of formation does not fit to the power-type dependence at longer exposures.

The studies of oxide film phase composition were performed by high-temperature X-ray diffraction method in order to find out the causes of the accelerated oxide film thickness growth at short exposures. The in-situ observation of the oxide film formation during the first 100 hours at 900 and 950 °C showed the formation of α -Al $_2$ O $_3$ and θ -Al $_2$ O $_3$ oxides on the surface (see Table 2).

The growth of α -Al $_2$ O $_3$ and θ -Al $_2$ O $_3$ at 950 °C as a function of time is given in Fig.3 as intensity curves $I_z(t)$. Both alumina phases on polished samples grow simultaneously in the first 50 hours and then the rate of θ -Al $_2$ O $_3$ growth decreases and α -Al $_2$ O $_3$ increases. The amount of θ -Al $_2$ O $_3$ reaches maximum after 100 hours and with further exposure the oxide starts to disappear as a result of its transformation into α -Al $_2$ O $_3$.

| Temperature, °C | Time, hr | | | | |
|-----------------|---|--|--|---|---|
| | 100 | 700 | 5000 | 10000 | 20000 |
| 900 | θ - + α -Al ₂ O ₃ | α -Al ₂ O ₃ | α -Al ₂ O ₃ | α -Al ₂ O ₃ | α -Al ₂ O ₃ (Me ₃ O ₄) |
| 950 | θ - + α -Al ₂ O ₃ | α -Al ₂ O ₃ | α -Al ₂ O ₃ | α -Al ₂ O ₃ (Me ₃ O ₄) | α -Al ₂ O ₃ , Me ₃ O ₄ |
| 1000 | α -Al ₂ O ₃ | α -Al ₂ O ₃ | α -Al ₂ O ₃ | α -Al ₂ O ₃ (Me ₃ O ₄) | α -Al ₂ O ₃ , Me ₃ O ₄ |

Table 2. Oxide film phase composition on Ni30Co28Cr10AlY and Ni30Co28Cr8AlY 200 μ m thick protective coatings (the phase indications in brackets mean, that their amount did not exceed 5 %).

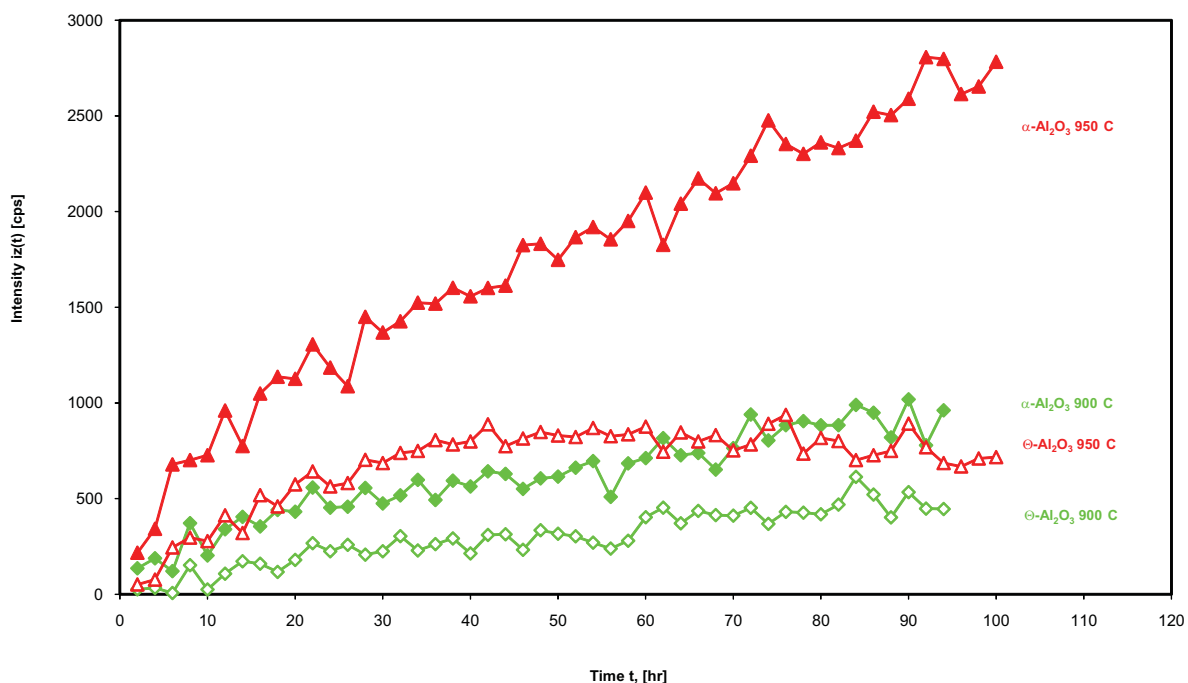


Fig. 3. Diffraction peak intensities of α -Al₂O₃ and θ -Al₂O₃ on polished coatings with 8% Al at 900°C and 950°C.

Hereinafter, these data were corrected in the developed model by splitting the oxide film growth curve into two parts (the first one refers to the period of simultaneous existence of θ -Al₂O₃ and α -Al₂O₃ oxides and the second – to period of only α -Al₂O₃).

Investigations using standard X-ray diffraction methods were performed in order to find out the oxide film growth mechanism in the range of $3 \cdot 10^2$ – $2 \cdot 10^4$ hours. It has been established that the oxide film phase composition in this range depends on aluminum content.

As is seen from Table 2, the oxide phase composition on coating with aluminum content over 8% (NiCoCr8AlY (for instance) after exposures in this time interval presents mainly α -Al₂O₃. At long exposures ($\geq 2 \cdot 10^4$ hours), an oxide of complex composition of a spinel type (Co,Ni)(Cr,Al)₂O₃ forms on the coating surface simultaneously with α -Al₂O₃. The results of the investigations performed enabled to plot the variation of the oxide film phase composition with time and temperature (Fig. 4).

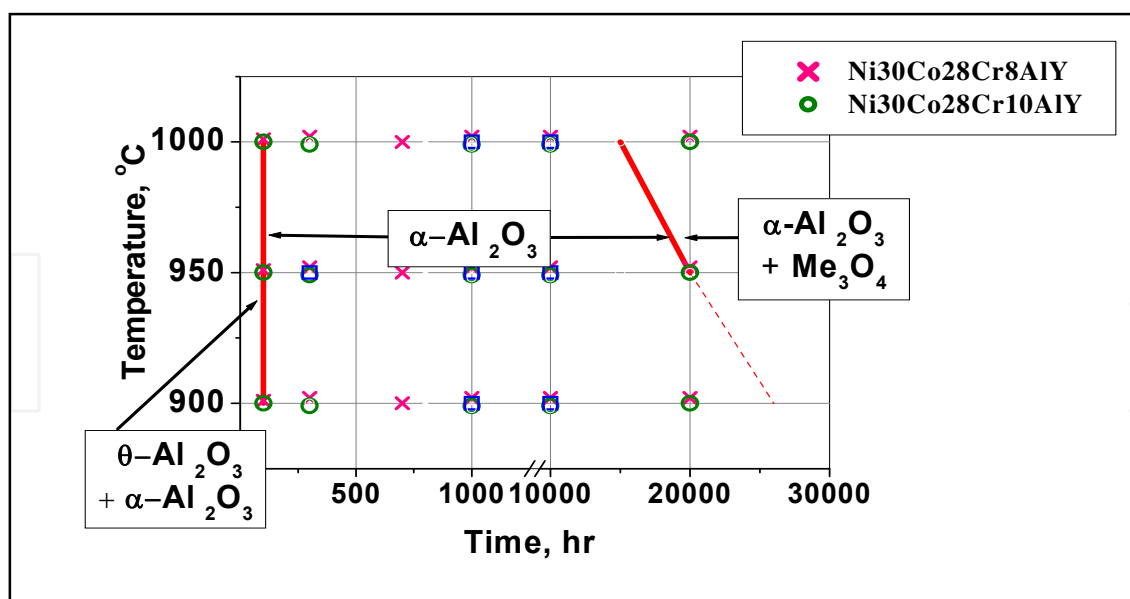


Fig. 4. Diagram of phase transformations in protective oxide film on Ni30Co28Cr8AlY and Ni30Co28Cr10AlY coating

Three areas can be seen on the diagram:

- θ - Al_2O_3 + α - Al_2O_3 corresponding to exposure time to 200 hours at all temperatures;
- α - Al_2O_3 corresponding to exposure time to $2 \cdot 10^4$ hours at all temperatures;
- α - Al_2O_3 + complex-composition oxide of a spinel type $(\text{Co,Ni})(\text{Cr,Al})_2\text{O}_3$ corresponding to exposure time over $2 \cdot 10^4$ at temperatures 950°C and above.

The basis for the development of methods of corrosion life modeling for these coatings was the existence of constant phase composition oxide (α - Al_2O_3) in a wide time range of exposures of Ni30Co28Cr8AlY and Ni30Co28Cr10AlY coatings for the temperature interval from 900 to 1000°C.

3.4.2 Kinetics of changes in coating structures

The coating structural changes and the redistribution of elements between a coating and a basic metal can be observed during long isothermal exposures of the coated basic metal. These changes depend on both boundary conditions including environment composition and the thickness and composition of an oxide film forming during long exposures and the thickness of a coating layer. Both the coating and basic metal compositions and the exposure times and temperatures will naturally determine the structural changes.

The work investigated the coating depth-variation of the chemical composition and structure and the changes in the surface layer of a basic metal during long exposures in air simulating service conditions in the medium of pure fuel combustion products. The structural changes in coating and surface layers of a basic metal and the thickness of the depleted layer were studied by optical metallography and the distribution of elements in the coating and basic metal layers – by X-ray spectrum analysis. The investigations have shown that all the coatings in their initial phase composition represent a matrix with a face-centered cubic lattice – γ -solid solution (Ni,Co) -Cr-based and a β -phase $(\text{Ni,Co})\text{Al}$ which is uniformly distributed across the coating layer. As is known, the β -phase presents a compensation reservoir for aluminum which is spent on the protective oxide film formation on a coating surface (Brady et al., 2001).

After applying a coating and performing heat-treatments a diffusion zone is formed in the alloy. The zone width, phase composition and structure depend on coating and basic metal compositions, coating application technique and subsequent heat-treatment conditions.

The diffusion zone for all the coatings had about the same width (a. 15 μm) and the phase composition a significantly different from that for basic metal $\gamma + \gamma'$ + carbides.

The characteristic structure of this coating after high temperature exposures is given in Fig.5.

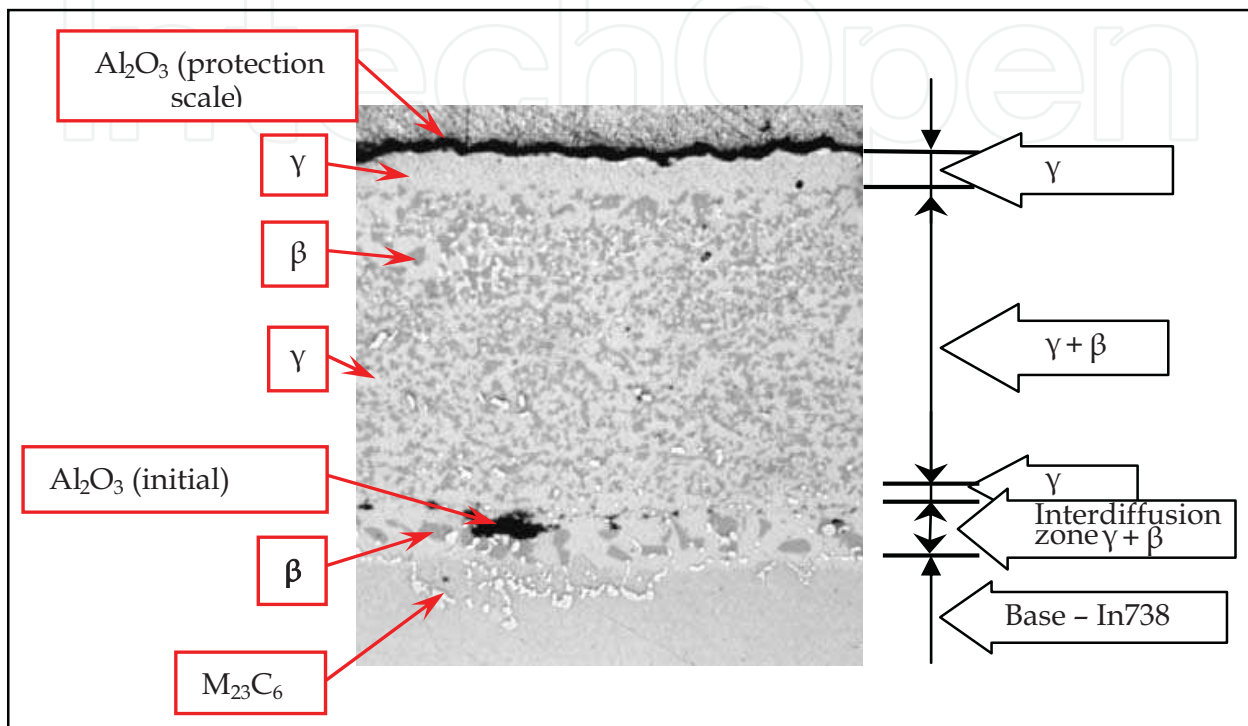


Fig. 5. Microstructure of Ni30Co28Cr8AlY coating on IN738LC alloy after exposure for 1000 hours at 950°C ($\times 300$)

During long-term exposures to high temperatures the coating structure changes due to the phase composition variation in its different zones followed by the formation of the characteristic layers.

It has been established that each of the coatings investigated after long-term exposures shows a specific character of structural changes.

The phase composition of the layers is mainly retained and their thickness changes with exposure time and temperature variation.

The changes in coating structure and phase composition depending on exposure time and temperature can be traced from the structures given in Fig.6.

It should be noted that the β -phase stabilization is observed in coatings of this composition. In relation to this, the phase transformation in a coating during its degradation at high-temperature exposure occurs in the direction $(\gamma + \beta) \rightarrow \gamma$.

The kinetics of a change in the volume fraction of the β -phase and aluminium concentration depending on exposure time and temperature can be seen from the curves in Fig.7 and 8.

The X-ray spectroscopy microanalysis of aluminium distribution in the surface layers of coatings in the initial state and after long exposure at 900 to 1000°C was performed. This microanalysis allowed to identify phases which had been found during metallographic study. The sizes of dealloyed and diffusion zones and special features of element

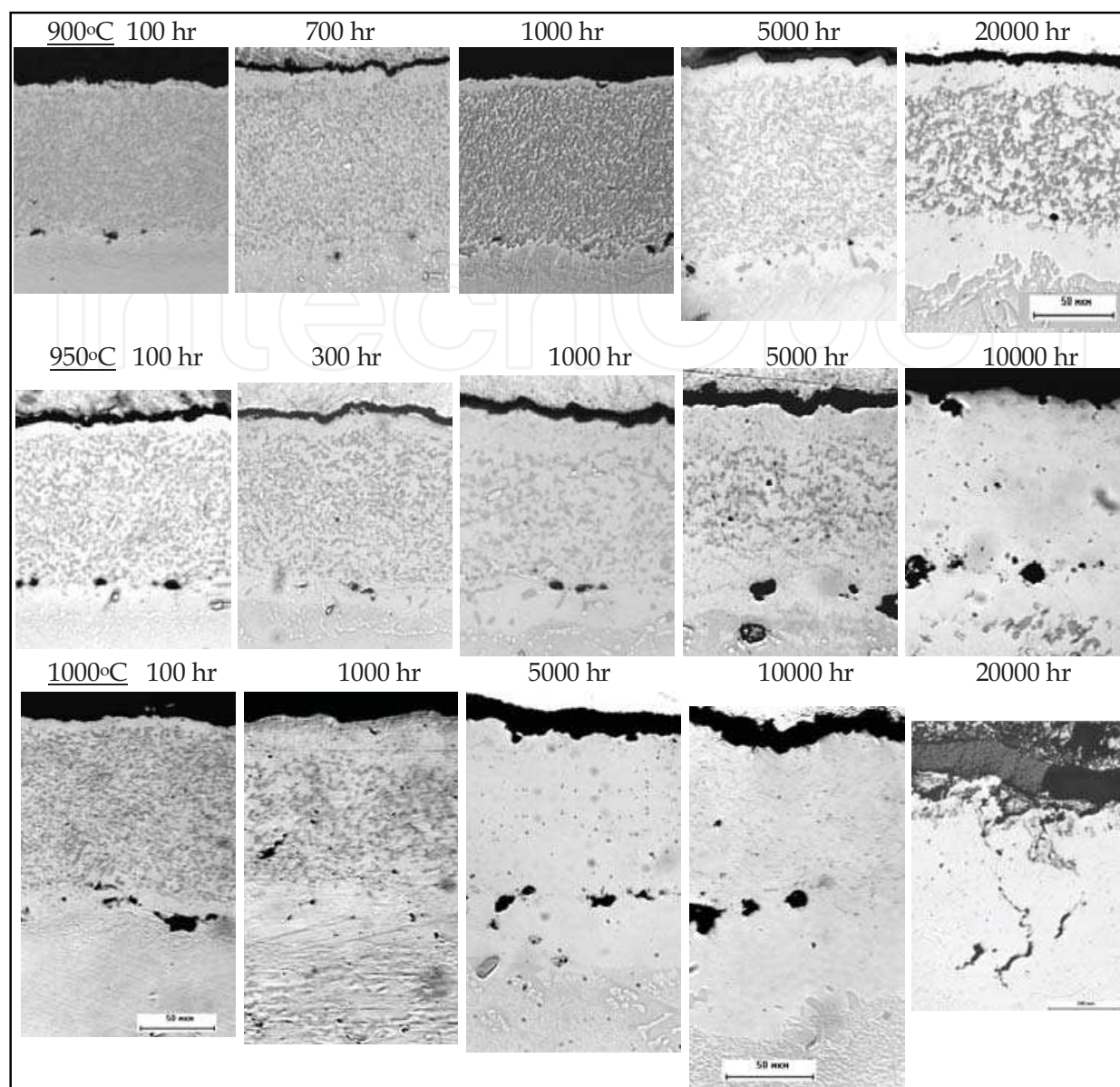


Fig. 6. The change in Ni₃₀Co₂₈Cr₈AlY coating on IN738LC alloy after different exposures at 900°C, 950°C and 1000°C

distribution in these zones can be seen from the curves built in Fig.7. Thus, for the external dealloyed zone characteristic for all types of coatings, a sharp decrease in aluminium content is observed under the oxide film Al₂O₃ (51.78%) up to 2.5 to 3.2%, which corresponds to its content in the γ -phase. In coatings of this composition, the volume fraction of the initial β -phase amount to 45% for the Ni₃₀Co₂₈Cr₈AlY coating and 62% for Ni₃₀Co₂₈Cr₁₀AlY. During the exposures this phase amount decreases according to the curves shown in Fig.8, the decrease being less intensive for the coating with greater aluminium content (and |or larger thickness) determining the coating aluminium life.

The diagrams of phase transformation proposed by Tamarin Jr. (Tamarin, 2002) are very convenient for presentation of data on the coating phase composition variation with exposure time and temperature. The external coating surface is taken as the onset of counting and considered to be constant in these phase transformation diagrams.

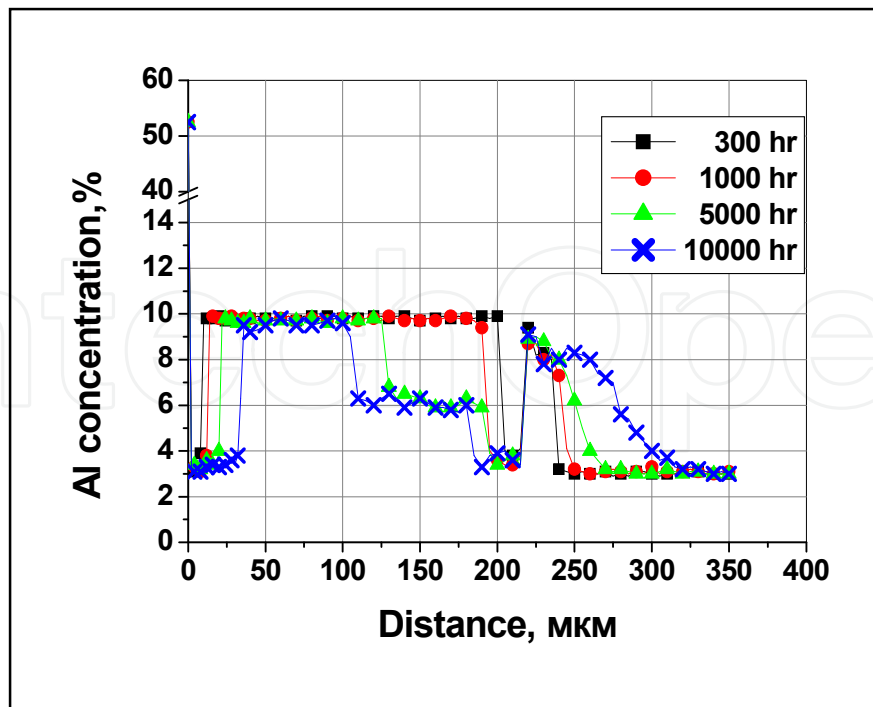


Fig. 7. The Al concentration profile across a coating after isothermal oxidation at high temperatures for up to 10 000 hour

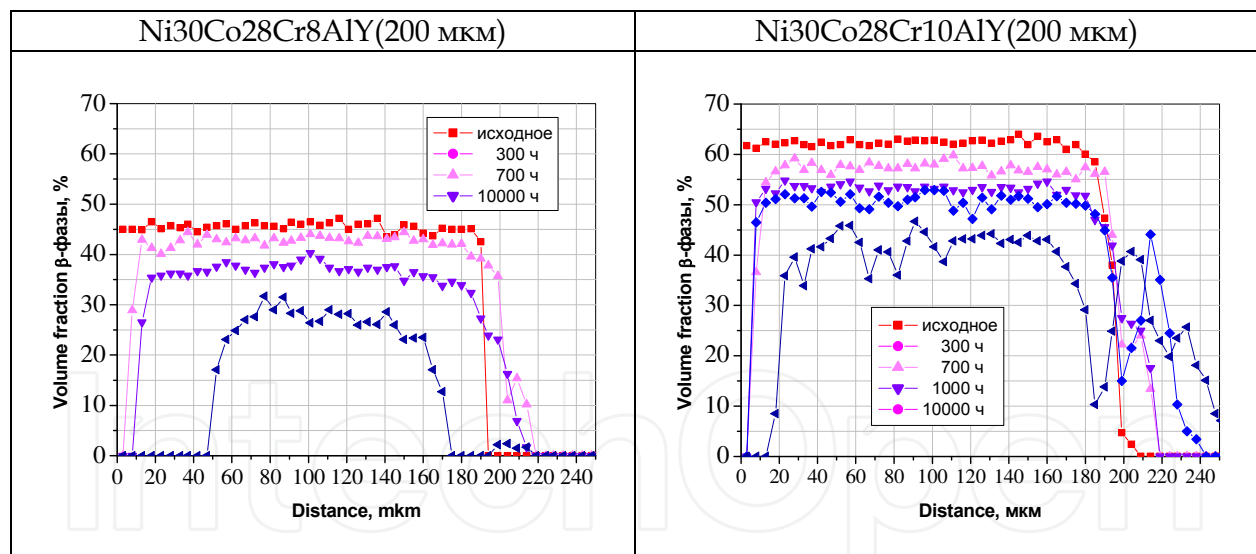


Fig. 8. The β -NiAl volume fraction in the $\gamma+\beta$ region after different duration of exposure at 950 °C

As is seen from Fig.9 and 10 the phase changes in external layers at high-temperature exposures are observed only due to the formation of an external depleted zone the width of which increases with increasing exposure time and temperature.

This zone is formed as a result of β -phase solution and aluminium consumption for the protective oxide film Al_2O_3 formation. At the same time, significant temperature-dependent structural changes of a diffusion zone are observed at the interface «coating - basic metal». The studies performed have found out particular features of the diffusion zone formation

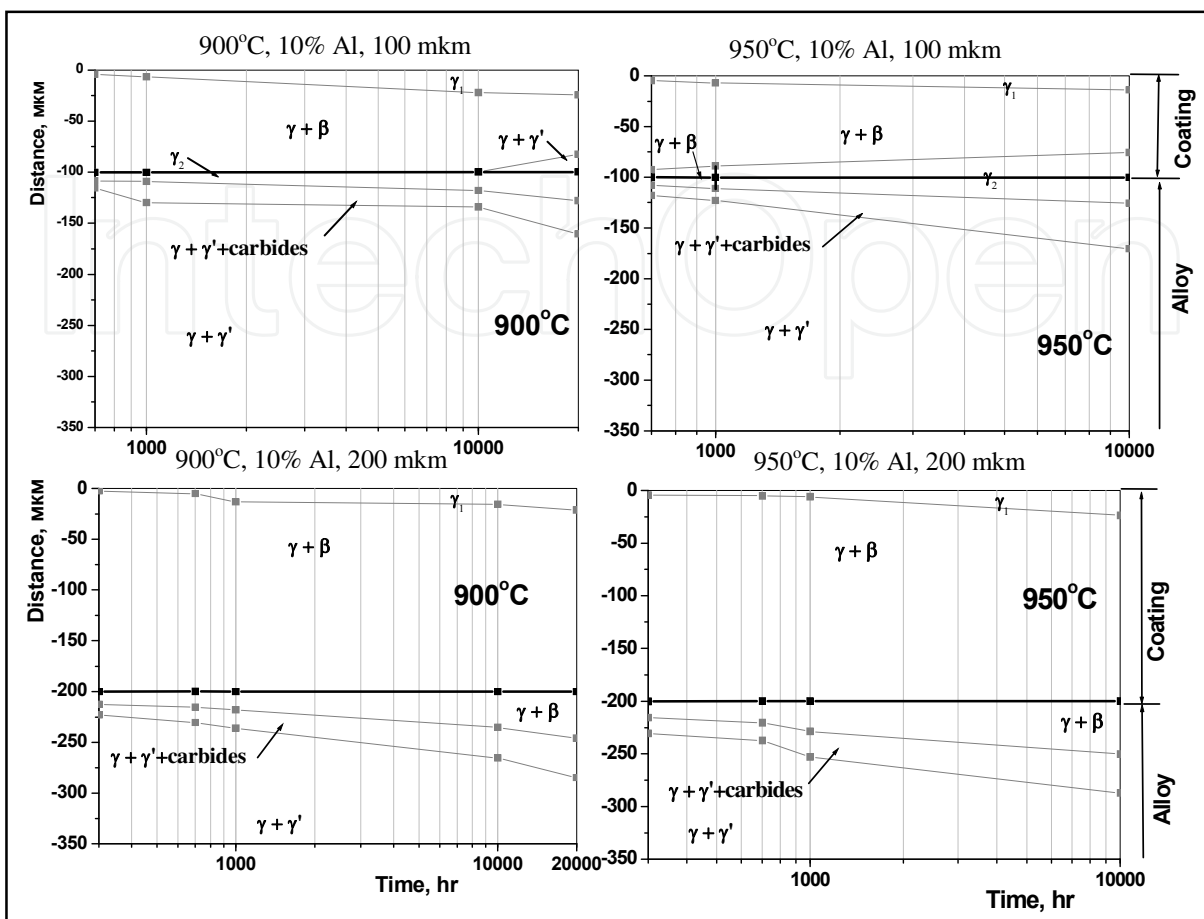


Fig. 9. Diagram of phase transformations in Ni30Co28Cr10AlY coating on IN738LC superalloy after exposure at 900 °C and 950 °C

between a metal and a coating depending on the aluminum content in the zone: with the aluminum content 10% the diffusion processes develop at the interface on a basic metal side (in this case a $\beta+\gamma$ structure is formed), while with the aluminum content 8% in a coating the diffusion processes develop on both sides of the interface (the $\beta+\gamma$ structure is first formed and then it transforms to a single γ -zone).

It is self-evident that the common model of the diffusion element redistribution in an oxide film, a coating and a basic metal requires accounting for the diffusion processes of all coating and alloy components. The practical handling the problem is however labour intensive, ambiguous, and requires a great number of experimental data.

That is why there is a good reason to make a choice of the best concept of diffusion which could be used as the basis of a coating corrosion life prediction according to one or another dominant process depending on the temperature interval.

In the temperature range 900 to 1000°C it is advisable to use aluminum redistribution processes whose characteristics have been studied as dominant diffusion processes for building a model.

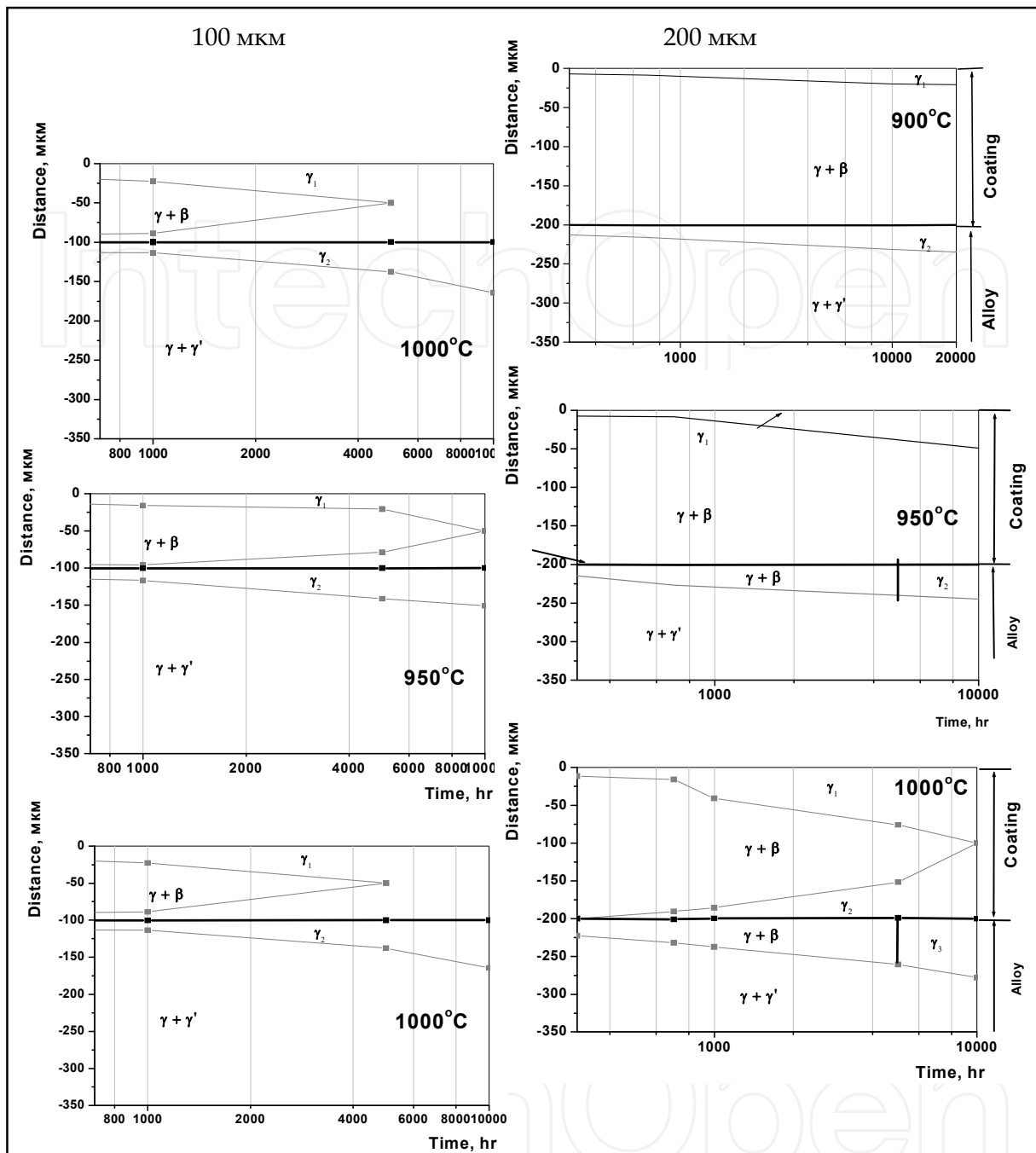
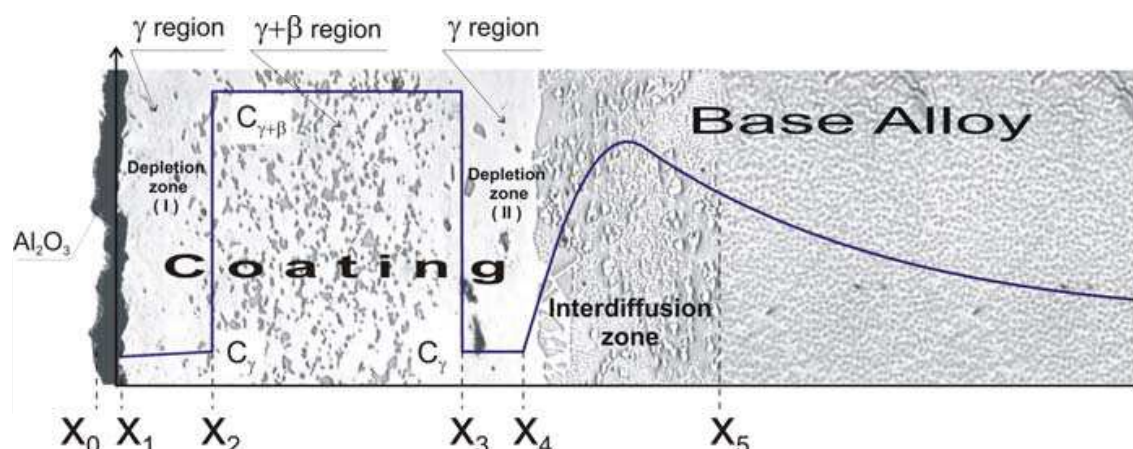


Fig. 10. The phase composition transformations in Ni₃₀Co₂₈Cr₈AlY coating (100µm and 200 µm on IN738LC superalloy after exposures at different temperatures (900 °C, 950 °C and 1000 °C).

4. Physical and mathematical models

The physical model for aluminium diffusion redistribution in the «oxide-coating-basic metal» system obtained from the analysis of experimental studies of oxidation and diffusion processes in coatings of NiCoCrAlY-type is described as follows (Fig.11).

An oxide is formed by combining aluminium and oxygen which is absorbed from the gaseous medium and by means of diffusion through the oxide layer $x_1 - x_0$ it reaches the interface



1. coating, 2. basic alloy, 3. γ -region, $\gamma + \beta$ region, 4. depletion zone, 5. interdiffusion zone

Fig. 11. Typical aluminium concentration distribution in an oxide, coating, and basic alloy.

x_1 oxide - coating. The aluminium diffusion from the coating proceeds in two directions:

- to the interface x_1 **oxide - coating** where it enters into reaction with the arrived oxygen.
- to the interface x_4 **coating - basic alloy** where it is accumulated in the interdiffusion zone and then diffuses to the basic alloy.

The formation of aluminium-depleted single-phase zones with a decreased Al (γ -phase) content on both the oxide and basic metal side (depletion zones I and II, Fig.11) occurs at the cost of the aluminium departure from the coating ($\gamma + \beta$ two phase zone. All aluminium leaving the coating departs from the coating ($\gamma + \beta$ two phase zone owing to the β -phase disappearance. The aluminium concentration profile has the form of a stepwise curve in the region of NiCoCrAlY coating and a curve with maximum in the interdiffusion zone within the basic alloy.

Six major zones can be distinguished:

- $x_0 < x < x_1$ oxide;
- aluminium-depleted $x_1 < x < x_2$ zone where only one γ -phase is present;
- two-phase $x_2 < x < x_3$ zone where γ - and β -phases exist simultaneously;
- $x_3 < x < x_4$ zone in the coating, also aluminium-depleted with γ -phase;
- interdiffusion aluminium-rich zone $x_4 < x < x_5$ in the basic alloy.
- $x_5 < x$ Zone in the basic metal where aluminium diffuses from the interdiffusion zone.

The aluminium accumulation in the interdiffusion zone with time occurs at the cost of the formation of different phases ($\gamma + \beta$ and $\gamma' + \beta$ -phases, for instance) due to the different quantitative compositions and the corresponding thermodynamical equilibrium of elements in a coating and a basic alloy. The accumulated in the interdiffusion zone aluminium diffuses partly to the basic alloy and back to the coating. In the model under consideration, all the borders apart from the border x_4 (the interface between a coating and a basic alloy) are movable. The borders x_2 and x_3 move toward each other because of the β -phase content decrease in the $\gamma + \beta$ -two-phase coating zone $x_2 < x < x_3$ from which the aluminium diffusion occurs. The concentrations of total aluminium amount of C and β -phase C_β in the $\gamma + \beta$ two-phase $x_2 < x < x_3$ decrease with time.

A mathematical model presented in [6] was taken as the basis of the above-described model. The model from [6] was improved by adding the capabilities of accounting for special features of border x_2 and x_3 moving as well as the formation and growth of the interdiffusion zone which has a great effect on the aluminium mass transfer processes in the coating-basic alloy system.

Below is given this improved model according to which aluminium mass transfer processes in the region of solution $x_1 < x < x_\infty$ can be described by the main diffusion equation

$$\frac{\partial C}{\partial \tau} = \frac{\partial}{\partial x} \left[D_{ef} \frac{\partial C}{\partial x} \right] + W \quad (2)$$

$\tau > 0, , x_1 < x < x_\infty, C = C(x, \tau), W = W(x, \tau), D_{ef} = D_{ef}(x), x_1 = x_1(\tau), x_2 = x_2(\tau), x_3 = x_3(\tau), x_5 = x_5(\tau),$
at the initial condition

$$C(x, 0) = C(x) = \begin{cases} C_n^0 & 0 < x < x_4 \\ C_{oc}^0 & x \geq x_4 \end{cases} \quad (3)$$

at the boundary condition on border x_∞

$$\frac{\partial C(x_\infty, \tau)}{\partial x} = 0 \quad (4)$$

and boundary condition on the movable border x_1 describing the aluminium diffusion flow from the coating to the left to form the oxide (Fig.11) at the cost of Al concentration gradient

$$J_{ox}(x_{1+}, \tau) = -D_{ef} \frac{\partial C(x_1, \tau)}{\partial x} \quad (5)$$

Flow (5) together with the mass (flow) $C(x_1, \tau) \frac{dx_1}{d\tau}$ that was formed owing to the border movement to the right make up a total oxide film mass of Δx thickness which can be described by two parabolic equation [5,6].

$$\Delta x(\tau) = x_1(\tau) - x_0(\tau) = \begin{cases} k_{ox}^* \cdot \tau^{0.5}, & 0 < \tau < \tau^* \\ k_{ox}^{**} \cdot \sqrt{\tau - \tau^0}, & \tau^* < \tau < \infty \end{cases} \quad (6), (7)$$

where k_{ox}^*, k_{ox}^{**} - intensity factors of oxide film thickness growth, in literature often called oxidation constants, τ^* - time prior to which the oxidation law (6) is valid and after which the oxidation law(6) is valid τ^0 -time prior to which the oxidation law (7) is in force.

At the moment of time τ^* the curves from equations (6) and (7) cross; τ^0 -the time (negative value) of crossing law (7) and the time axis τ . The necessity of describing the law of Al oxide growth by the two parabolic equations (6) and (7) is due to a more rapid growth of oxide θ -phase prior to the moment of time τ^* and a slower growth of α - phase of the oxide film Al_2O_3 at $\tau > \tau^*$. The factors $k_{ox}^*, k_{ox}^{**}, \tau^0$ and the τ^* value in (6) and (7) are determined from the experimental data on the oxide film thickness growth with time.

The border x_1 movement is described by the equation

$$\frac{dx_1}{d\tau} = 0.5 \frac{k_{Al_2O_3}}{\left(1 + \frac{1}{s}\right)} \frac{\rho_{Al_2O_3}}{\rho_n} \frac{1}{\sqrt{\tau}}$$

derived with regard to the stoichiometric relationship between Al and oxygen masses consumed to form an aluminium oxide. The relationship is used in the model of parabolic law of oxide film thickness growth (6.7).

According to the accepted model prototype [6] the following concentration values are set on movable borders x_2 and x_3 :

$$C(x_{2-}, \tau) = C(x_{3+}, \tau) = C_\gamma, \quad C(x_{2+}, \tau) = C(x_{3-}, \tau) = C_{\gamma+\beta}. \quad (8)$$

Then by analogy with the boundary condition (5) for a movable border x_4 we can write the aluminium diffusion flow from a coating to the right to form the interdiffusion zone $\Delta y = x_5 - x_4$ and aluminium diffusion to a basic metal as

$$J_b(x_{4-}, \tau) = -D_{ef} \frac{\partial C(x_{4-}, \tau)}{\partial x} \quad (9)$$

In compliance with the physical model (Fig.2) the aluminium flow (9) arrived from the coating takes part in the formation of new phases in the interdiffusion zone $\Delta y = x_5 - x_4$ thick and uniformly segregates in this zone, that is

$$J_b(x_{4-}, \tau) = W(x, \tau) \cdot \Delta y(\tau) \quad (10)$$

where the interdiffusion zone width $\Delta y = x_5 - x_4$ increase with time due to the border x_5 movement to the right and the parabolic law of its growth, as for the oxide film, is taken in the form of

$$\Delta y(\tau) = x_5(\tau) - x_4 = k_{iz} \cdot \sqrt{\tau - \tau_{iz}^0} \quad (11)$$

k_{iz} factors and τ_{iz}^0 value in (11) are determined from the experimental data on the interdiffusion zone growth with time. The expression for Al W mass arrived from the coating and uniformly segregated in the interdiffusion zone $x_4 < x < x_5$ is taken as dependent on $C_{\gamma+\beta} - C_\gamma$ (in power m) and has the form

$$W = W(x, \tau) = \begin{cases} k_w \cdot (C_{\gamma+\beta} - C_\gamma)^m, & x_4 < x < x_5 \\ 0, & x_1 < x < x_4, \quad x > x_5 \end{cases} \quad (12)$$

where k_w -intensity factor of aluminium segregation in the interdiffusion zone. Since the balance of masses must be met in the coating-oxide film-basic alloy system the expression for the total aluminium flow departed from the coating two-phase zone, in accord with (5) and (9), will take the form

$$J_\Sigma(\tau) = J_{ox}(x_{1+}, \tau) + J_b(x_{4-}, \tau) \quad (13)$$

In accord with the accepted physical model all aluminium flowing from the coating departs the coating $\gamma+\beta$ two-phase zone at the cost of β -phase consumption. Then the movement of borders x_2 and x_3 as well as the aluminium concentration decrease in the $\gamma+\beta$ two-phase zone can be described by the equation of mass balance between aluminium mass flows on these borders and the flows resulted from the aluminium concentration difference in $\gamma+\beta$ - and γ - phases $\Delta C = C_{\gamma+\beta} - C_\gamma$

$$J_{\Sigma} = J_{\gamma}(x_{2-}, \tau) + J_{\gamma}(x_{3+}, \tau) = \Delta C \cdot \frac{dx_2}{d\tau} + \Delta C \cdot \frac{dx_3}{d\tau} + (x_3 - x_2) \frac{dC_{\gamma+\beta}}{d\tau} \quad (14)$$

where

$$J_{\gamma}(x_{2-}, \tau) = -D_{ef} \frac{dC(x_{2-}, \tau)}{dx} \text{ and } J_{\gamma}(x_{3+}, \tau) = -D_{ef} \frac{dC(x_{3+}, \tau)}{dx}$$

are diffusion flows to the oxide and basic alloy due to the aluminium concentration gradients to the left and to the right of borders x_2 and x_3 respectively. After division of all the terms by J_{Σ} the expression (14) has form

$$1 = \Delta C \cdot \frac{dx_2}{d\tau} / J_{\Sigma} + \Delta C \cdot \frac{dx_3}{d\tau} / J_{\Sigma} + (x_3 - x_2) \frac{dC_{\gamma+\beta}}{d\tau} / J_{\Sigma} = g_2 + g_3 + g_{2,3} \quad (15)$$

where

g_2 and g_3 – total aluminium mass fractions gone from the coating due to the movement of borders x_2 and x_3 respectively, $g_{2,3} = (1 - g_2 - g_3)$ – a fraction of aluminium mass gone from the coating due to the Al β -phase amount decrease in the $x_2 < x < x_3$ zone.

The g_2 and g_3 quantities having a direct effect on the rate of borders x_2 and x_3 movement are also taken as dependent on the concentration difference $\Delta C = C_{\gamma+\beta} - C_{\gamma}$

$$g_2 = k_2 \cdot \frac{\Delta C}{C_n^0}, \quad g_3 = k_3 \cdot \frac{\Delta C}{C_n^0} \quad (16)$$

The laws of borders x_2 and x_3 movement and Al $C_{\gamma+\beta}$ amount decrease in a two-phase zone can be derived from expressions (15) and (16)

$$\frac{dx_2}{d\tau} = J_{\Sigma} \frac{k_2}{C_n^0}, \quad \frac{dx_3}{d\tau} = J_{\Sigma} \frac{k_3}{C_n^0}, \quad \frac{dC_{\gamma+\beta}}{d\tau} = J_{\Sigma} (x_3 - x_2) (1 - g_2 - g_3) \quad (17)$$

The k_2 and k_3 coefficients of proportionality in (16) are determined from expressions (16) and (17) based on the experimental data on the dynamics of borders x_2 and x_3 movement and the value of platform $C_{\gamma+\beta}$ in the region $x_2 < x < x_3$ for different sample exposure times. The association of total Al $C_{\gamma+\beta}$ content with the β -phase $C_{\beta}(\tau)$ amount in the coating is described by the expression

$$C_{\gamma+\beta}(\tau) = C_{\beta}(\tau) \cdot C_{\beta}^{Al} + [1 - C_{\beta}(\tau)] \cdot C_{\gamma} \quad (18)$$

where

$C_{\beta}^{Al} = const$ is Al amount in β -phase.

The diffusion factor D_{ef} , k_w factor and the index of power m in the mathematical model (2) - (18) are determined from the experimental data by solving the inverse problem of diffusion. The diffusion factor D_{ef} in (2) is valid for all the region of solution except for the subregion $x_2 < x < x_3$ where it was taken to be equal to a large value because of the lack of a space aluminium concentration gradient. The accumulated in the interdiffusion zone aluminium

diffuses partly back to the coating as a result of the aluminium concentration gradient to the right of the borders x_4

The appearing here diffusion flow

$$J_{iz}(x_{4+}, \tau) = -D_{ef} \frac{\partial C(x_{4+}, \tau)}{\partial x}$$

returns to the interdiffusion zone by adding to the main flow (9).

The distinction of the above model from that in [6] is not only in the account for the interdiffusion zone but also in the introduction of total aluminium mass fractions g_2 and g_3 in (15) which departed the coating due to the movement of borders x_2 and x_3

This allow for a wider application of the model (2) -(18) to different coating compositions for which the rate of movement is not defined on the whole by concentration gradients on borders x_2 , x_3 and x_4 . In term of the thermodynamic theory of diffusion, these borders can be determined by complex processes of the β and γ phase formation dissolution in a solid solution, but the practical application of this theory for complex systems under consideration is rather conjectural. Following assumptions are accepted in this model:

- the character of main physical-chemical processes occurring in the «coating-substrate» system does not change with time;
- only one element (Al) takes part in the formation of an oxide. This assumption for the coating type at hand is conformed by experimental investigations for up to 20000 hours
- the oxide forms on the border x_1 only;
- aluminium comes to the interdiffusion zone only from a coating ;
- the diffusion factor D_{ef} derived by the IPD solution is an effective characteristic independent of time;
- the formation of new phases at the interface coating-basic alloy is not accounted for;
- no oxide film spallation takes place.

The above formulated mathematical model of diffusion and oxidation processes is integrated by means of the numerical method of finite differences using the inexplicit diagram and iterative method of nonlinearity accounting.

5. Calculation results

The application of calculation and experimental approach to the analysis of aluminium, oxidation and diffusion processes in a coating 100 μm thick is considered. The coating contains Ni35%, Co30%, Cr24% and Al8.4% (here and below the concentration is given in weight percents unless otherwise specified).

The mathematical model (2) -(18) was used in calculations. The above described calculation-experimental approach was used for experimental conditions at 950°C and exposures for 700, 10000 and 20000 hours. The model parameter identification was performed with the use of exposure for 700 and 10000 hours (Fig.12a, 12b). The results of Al and β -phase concentration distribution prediction were compared to the results of experimental exposure for 20000 hours (Fig.12b).

The main input parameters in the model (2) -(18) were diffusion factors D_{ef} , intensity factor of aluminium segregation in the interdiffusion zone k_w , the index of power m , weight coefficients k_2 , k_3 and coefficients k_{ox}^* , k_{ox}^{**} , and τ^0 . The coefficients k_{ox}^* , k_{ox}^{**} , and τ^0 in the parabolic equations(6,7) were found by the approximation of experimental data $\Delta x_{ex} = f(\tau)$

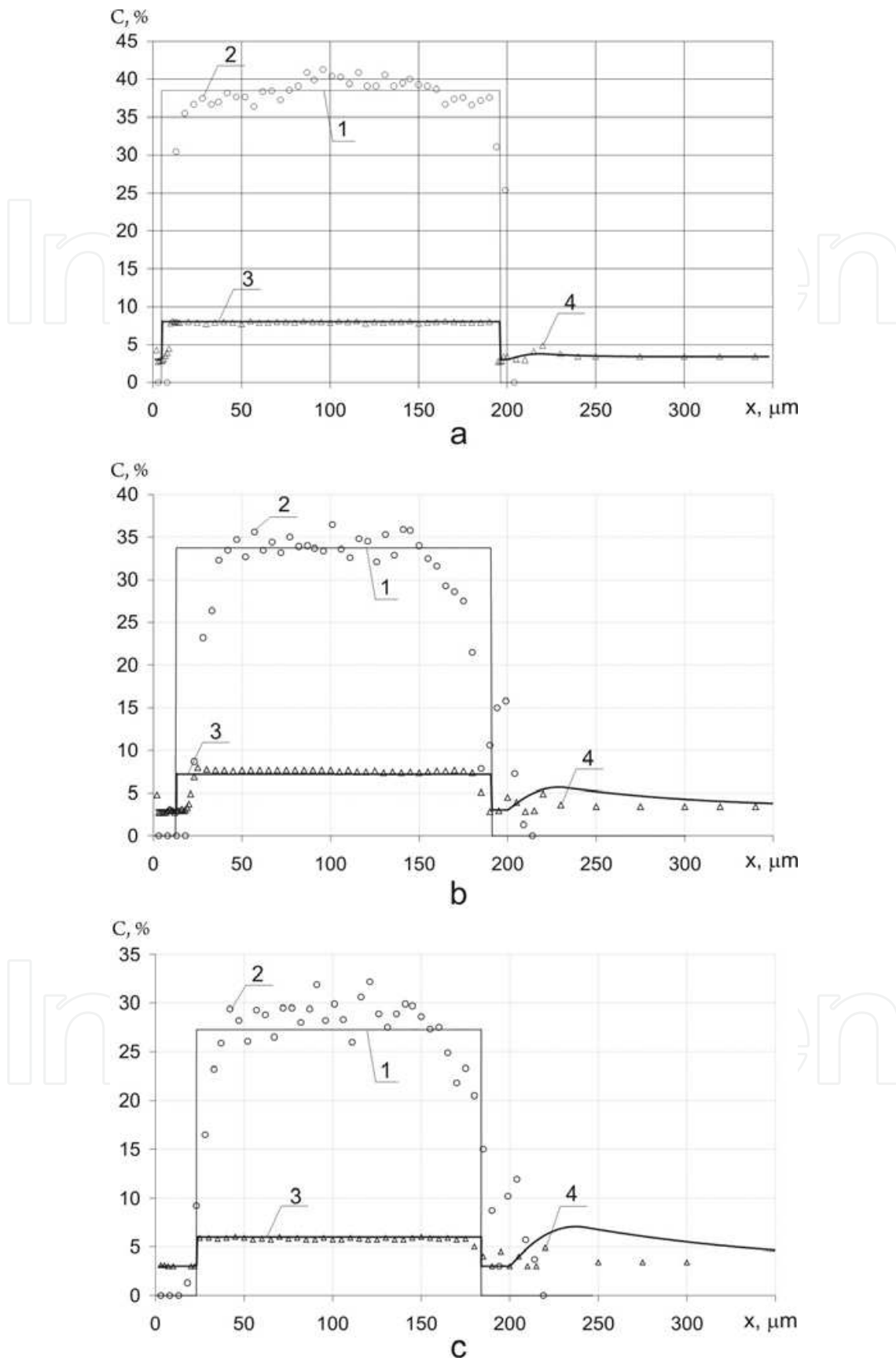


Fig. 12. Comparison of calculated and measured concentration profiles

for exposures 7000 and 10000 hours. In our case for the temperature 950°C $k_{ox}^* = 2.88 \cdot 10^{-9}$ m/s^{0.5}, $k_{ox}^{**} = 7.44 \cdot 10^{-10}$ m/s^{0.5}, $\tau^0 = -3.3 \cdot 10^7$ s.

The weight coefficients were preestimated from the analysis of experimental data $k_2=0.24$, $k_3=0.16$.

The diffusion factor D_{ef} , the intensity factor of aluminium segregation in the interdiffusion zone k_w and the index of power m were found by IPD solution. The initial values of these factors were taken as follows: $D_{ef}=1.0 \cdot 10^{-15}$.m²/s, $k_w = 1.0 \cdot 10^{-8}$ s⁻¹, $m = 0.5$.

The IPD solution was performed by the method described in more detail in [10]. The parameter values found by using the IPD solution were $D_{ef}=7 \cdot 10^{-16}$.m²/s, $k_w = 1.37 \cdot 10^{-7}$ s⁻¹, $m = 0.65$.

The index of power appeared to be constant $m = 0.65$ for all three temperatures in the experiments. The C_γ value was taken from the experiment as equaling 3.0%.

It is commonly assumed that the time of a complete β - phase dissolution is a NiCoCrAlY-type coating life. This criterion is determined by the fact that after the β - phase disappearance the aluminium concentration in a coating is not sufficient for maintaining the protective oxide film formation. Further operation of the coating with the dissolved β - phase brings to the rapid oxidation of blade coating and basic alloy layers, which is impermissible.

The calculation results of the time of β - phase disappearance in the coating for three temperatures 900, 950 and 1000°C are given in Fig.13.

Thus with the above criterion of coating lifetime in mind a lifetime of NiCoCrAlY-type coating with the initial Al amount 8.4% and 20µm thick is considered to be 50 thousand hours at 900°C, 22 thousand hours at 950°C and 12.5 thousand hours at 1000°C.

By using defined model parameters the corrosion lifetime of different coatings was assessed in comparison with the obtained experimental data (Fig.14, Table3).

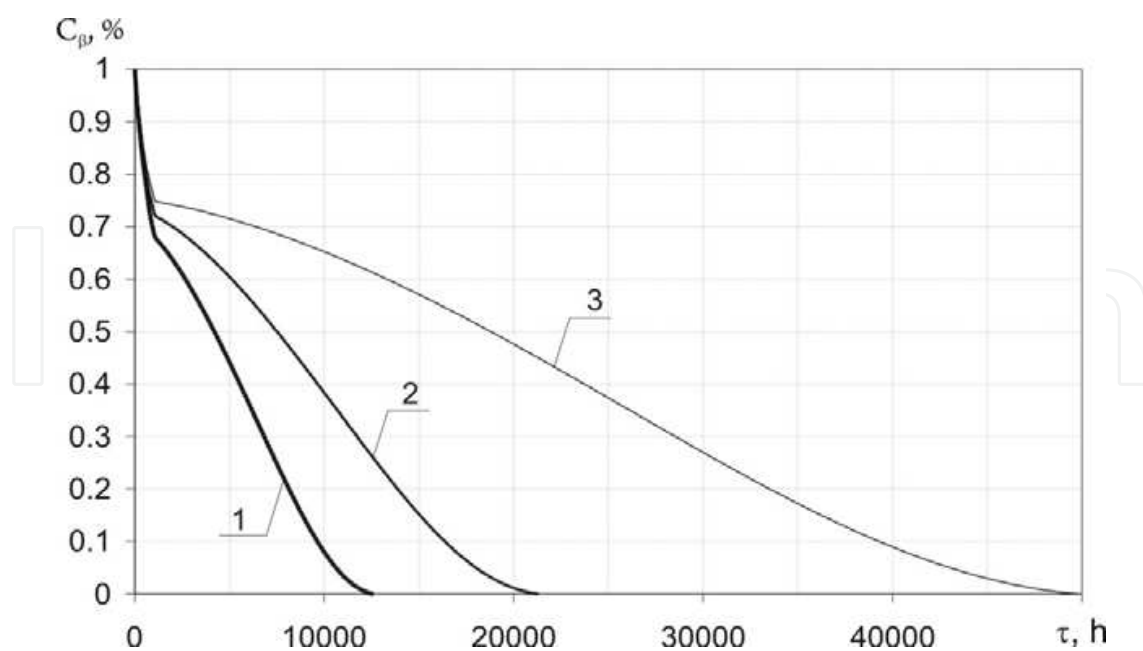
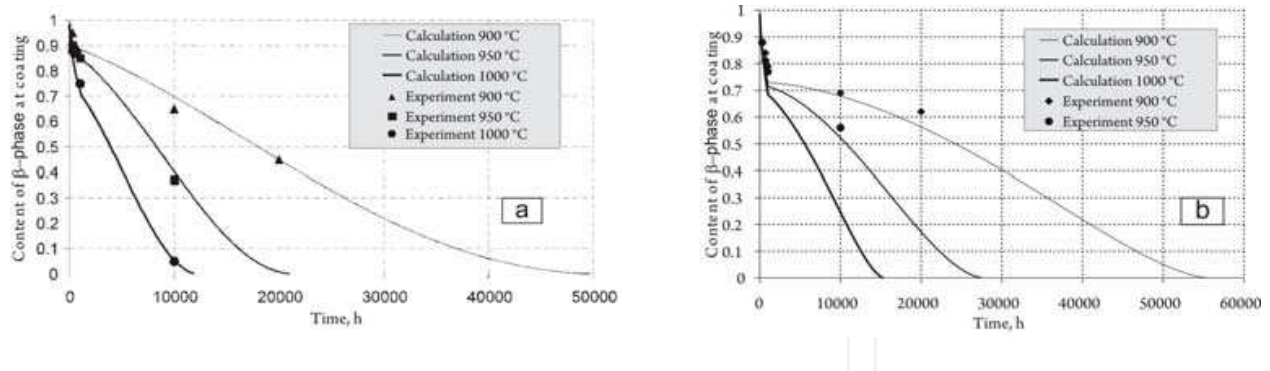


Fig. 13. B-phase C_{β} (volume %) concentrations in a coating depending on time 1- at $T=1000^{\circ}\text{C}$, 2- at $T=950^{\circ}\text{C}$, 3 - at $T=900^{\circ}\text{C}$



- a- Ni30Co28Cr8AlY 200µm thickness on In738LC alloy,
- b- Ni30Co28Cr10AlY 200µm thickness on IN738LC alloy.

Fig. 14. The life of different coatings determined from the β -phase amount (volume %) versus time curves for coatings

| Coating (base alloy) | Calculated coating life time (h) at temperature, °C | | | |
|--|---|-------|-------|-------|
| | 900 | 950 | 980 | 1000 |
| Co29Cr6AlY (GS6K) | 11400 | 5000 | - | 1000 |
| Ni30Co28Cr8AlY (100 µm) (IN738 LC) | - | 12500 | - | - |
| Ni30Co28Cr8AlY (200 µm) (IN738 LC) | 49000 | 21000 | - | 12000 |
| Ni30Co28Cr10AlY (100 µm) | - | - | - | - |
| Ni30Co28Cr10AlY (200 µm) (IN738 LC) | 55000 | 28000 | - | - |
| Ni25Cr5Al2SiTaY (CM 247 LC) | 46000 | 26000 | - | 8000 |
| Ni25Co17Cr10AlYRe (Rene80) | 58000 | 34000 | - | 11500 |
| Ni25Co17Cr10AlYRe (LPPS) (PWA1483 SX) | - | 51400 | - | 22800 |
| Ni25Co17Cr10AlYRe (VPS) (PWA1483 SX) | 52700 | - | 20000 | - |

1 -coating (on alloy), 2 - Calculated coating life (hour at temperature., 3 -on

Table 3. The results of different coating life calculations

6. Conclusions

The proposed calculation and experimental approach has shown its efficiency in lifetime assessments of gas turbine blade coatings. The model taken from [6] was significantly improved.

The existence of the interdiffusion zone was modeled and calculated and a more flexible approach to the calculation for two-phase border movement was introduced in the mathematic model as a result of model improvement.

There is a good agreement between experimental and calculated aluminium concentration profiles and β - phase amount in a coating.

The application of the approach made it possible to evaluate model input parameters, in particular, to determine aluminium diffusion factor and perform rotating blade life predictions.

The authors express their acknowledgement to the NATO Scientific Program, Ministry of Education and Science and the Institute of Engineering Thermal Physical, Ukraine for the financial support of the researches; to Alperine S. (SNECMA, France), Stamm W. (SIEMENS, Germany) for their participation in discussing the results of the work.

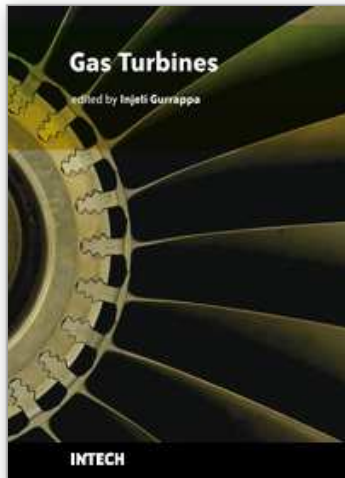
7. References

- P. Kolomyteev, Gaseous corrosion and strength of nickel alloys | | M.: Metallurgy, 1984, – p.216.
- N. Nikitin, Metal heat-resistance calculation. M.: Metallurgy, 1989, – p.207.
- Superalloys II, edited by Ch. Sims, N. Stoloff, W. Hagel. Book 2. M.: Metallurgy, 1995, – p.384.
- Meirer S. M., Nissleu D. M. , Sheffer K. D. , Cruse T. A., Thermal Barrier Coating Life Prediction Model Developed | | Trans. of ASME. J. of Eng. For Gas Turbines and Power, 1992, v116, №4, p. p. 250-257.
- J. Nesbitt, Numerical Modelling of High-Temperature Corrosion Processes/ | | Oxidation of metals, 1996, 44, p. p. 309-338.
- E.Y. Lee, D. M. Chartier, R. R. Biederman and K. D. Sisson, Modelling the microstructural evolution of M-Cr-Al-Y coatings during high-temperature oxidation. | | Surface and coatings technology, 1987, 32. p.p. 19-39.
- J. Nesbitt, R. Heckel, Interdiffusion in Ni-rich, Ni-Cr-Al Alloys at 1100 and 1200°C: Part II. Diffusion coefficients and Predicted Concentration Profiles | | Met.Trans., 1987, 18A,December, p.p. 2087-2094.
- E. Kartavova, P. Krukovsky, Modelling of Heat Transfer Processes in protective coatings of GT blades: | | Industrial Heat Engineering,1996.№6, p.p. 23-30.
- P. Krukovsky, V. Kolarik, K. Tadya, A. Rybnikov, I. Kryukov, M. Jues-Lorento, Lifetime Modelling of High Temperature Corrosion Processes. | | Proceedings of an EFC Workshop, 201, p.p. 231-245.
- P. Krukovsky, Inverse Problems of Heat Transfer (general engineering approach) – Kiev, Institute of Engineering Thermal Physics NaN Ukraine, 1998. – p.218.
- K. Borggreen, P. Auerkari, Assesment of the thermal damage in the superalloy GTD – Baltika V. , Condition and Life Management for Power Plants, vol. 1, 2001, p.p. 125-137.

- Brady M. P. , Pint B. A., Tortorelli P. F., Whright, Hanrahan R. J. High-temperature oxidation and corrosion of intermetallic || Corrosion and environmental degradation, edited by M. Schutze || v. II, Ch. 6, 2001 – p.p. 229-311.
- Tamarin Y. Protective coating for turbine blades || ASM International, Materials Park, ON, 2002, p.247.

IntechOpen

IntechOpen



Gas Turbines

Edited by Gurrappa Injeti

ISBN 978-953-307-146-6

Hard cover, 364 pages

Publisher Sciyo

Published online 27, September, 2010

Published in print edition September, 2010

This book is intended to provide valuable information for the analysis and design of various gas turbine engines for different applications. The target audience for this book is design, maintenance, materials, aerospace and mechanical engineers. The design and maintenance engineers in the gas turbine and aircraft industry will benefit immensely from the integration and system discussions in the book. The chapters are of high relevance and interest to manufacturers, researchers and academicians as well.

How to reference

In order to correctly reference this scholarly work, feel free to copy and paste the following:

P. Krukovskyi, K. Tadya, A. Rybnikov, N. Mozhajskaja, I. Krukov and V. Kolarik (2010). Life Time Analysis of MCrAlY Coatings for Industrial Gas Turbine Blades (Calculational and Experimental Approach), Gas Turbines, Gurrappa Injeti (Ed.), ISBN: 978-953-307-146-6, InTech, Available from:
<http://www.intechopen.com/books/gas-turbines/life-time-analysis-of-mcraly-coatings-for-industrial-gas-turbine-blades->

INTECH
open science | open minds

InTech Europe

University Campus STeP Ri
Slavka Krautzeka 83/A
51000 Rijeka, Croatia
Phone: +385 (51) 770 447
Fax: +385 (51) 686 166
www.intechopen.com

InTech China

Unit 405, Office Block, Hotel Equatorial Shanghai
No.65, Yan An Road (West), Shanghai, 200040, China
中国上海市延安西路65号上海国际贵都大饭店办公楼405单元
Phone: +86-21-62489820
Fax: +86-21-62489821

© 2010 The Author(s). Licensee IntechOpen. This chapter is distributed under the terms of the [Creative Commons Attribution-NonCommercial-ShareAlike-3.0 License](#), which permits use, distribution and reproduction for non-commercial purposes, provided the original is properly cited and derivative works building on this content are distributed under the same license.

IntechOpen

IntechOpen